



Published in final edited form as:

Biochemistry. 2011 June 28; 50(25): 5799–5805. doi:10.1021/bi2003923.

The Influence of Histidine Tag Attachment on Picosecond Protein Dynamics†

Megan C Thielges⁺, Jean K. Chung⁺, Jun Y. Axup[#], and Michael D. Fayer^{+,*}

⁺Department of Chemistry, Stanford University, Stanford, CA 94305

[#]Department of Chemistry and the Skaggs Institute for Chemical Biology, The Scripps Research Institute, La Jolla, CA 92037

Abstract

Poly-Histidine (His) affinity tags are routinely employed as a convenient means of purifying recombinantly expressed proteins. A tacit assumption is commonly made that His tags have little influence on protein structure and function. Attachment of a His tag to the N terminus of the robust globular protein myoglobin leads to only minor changes to the electrostatic environment of the heme pocket, as evinced by the nearly unchanged FT-IR spectrum of CO bound to the heme of His-tagged myoglobin. Experiments employing 2D IR vibrational echo spectroscopy of the heme bound CO, however, find that significant changes occur to the short time scale (ps) dynamics of myoglobin as a result of His tag incorporation. The His tag mainly reduces the dynamics on the 1.4 ps timescale and also alters protein motions of myoglobin on the slower, >100s ps timescale, as demonstrated by the His tag's influence on the fluctuations of the CO vibrational frequency, which reports on protein structural dynamics. The results suggest that affinity tags may have effects on protein function and indicate that investigators of affinity tagged proteins should take this into consideration when investigating the dynamics and other properties of such proteins.

Affinity tags have greatly eased the difficulty of obtaining high quantities of purified proteins for biophysical and biochemical studies.(1-3) While a variety are available, ranging from large protein fusions to short peptide sequences, the poly-Histidine tag (His) tag is the most widely utilized.(4) It involves the introduction of only a short, frequently six, His sequence that enables the purification of proteins by metal affinity chromatography. The affinity tags may be optionally removed by the insertion of a protease recognition sequence; however, the reactions often show low efficiency, require large quantities of costly enzymes, introduce an additional purification step for protease removal, and can lead to side reactions at unwanted protein sites.(5-7) Due to these drawbacks, His tags are frequently retained.(8-12) The addition of a His tag is commonly assumed to result in negligible perturbation to the protein structure and function. While evidence suggests this is often true,(13) in some cases His tag introduction has caused alterations in protein structure or interference with binding interactions.(14-23)

A His tag was introduced for facile purification of recombinant sperm whale myoglobin (His₆Mb), perhaps the most extensively studied protein, which reversibly binds oxygen and other small polyatomic molecules (Figure 1). When CO is bound to Mb (MbCO) and other

†This work was supported by the National Institutes of Health (2-R01-GM061137-09). MCT acknowledges the NIH for a NRSA postdoctoral fellowship (F32-GM090549).

*fayer@stanford.edu Phone: 650-723-4446. Fax: 650-723-4817.

Supporting Information **Available**: Multiexponential fits to the MbCO CLS decay, CD and UV/visible spectra of His₆MbCO. This material is available free of charge via the Internet at <http://pubs.acs.org>.

heme proteins, its IR absorption is intense and highly sensitive to the protein electrostatic environment.(24-31) Because of this the IR spectrum of CO has long been analyzed for characterization of heme protein conformations and for identification of features of the heme pocket environment that may be associated with function.(24, 25) In addition to its use in structural studies, the CO vibration provides a convenient probe for measuring the dynamics in heme proteins.(12, 30, 32-36) Protein structural fluctuations throughout the protein lead to corresponding fluctuations in the CO vibrational frequency. The technique of 2D IR vibrational echo spectroscopy can be used to measure the timescales and amplitudes of these frequency fluctuations, and thus characterize the dynamics of the CO's protein environment. MbCO in particular has been a workhorse for our development of 2D IR vibrational echo spectroscopy for the study of dynamics in proteins.(37-47)

Due to the high sensitivity of the CO vibrational spectrum to protein structure, particularly in or near the heme pocket, any large perturbation to the Mb structure as a result of His tag introduction should lead to significant changes in the CO spectrum. Very little change is observed in the FT-IR spectrum of MbCO upon introduction of the His tag, suggesting the placement of the His tag at the N-terminus of Mb, located far from the heme pocket and bound CO (Figure 1), has little influence on the heme pocket structure of such of robust, globular protein. Here we report a comparison of the picosecond timescale dynamics of the MbCO and His₆MbCO measured with 2D IR vibrational echo spectroscopy. Although the CO vibrational spectrum is virtually unchanged with the addition of the His tag, the dynamics of His₆MbCO differ significantly from those of the untagged protein. These results underscore the care that must be taken in studies of the dynamics and other biophysical properties of His-tagged proteins, particularly with spectroscopic techniques that are sensitive to protein structural fluctuations.

II. Experimental Procedures

Sperm whale Mb with an N-terminal His₆ tag and TEV cleavage site (MGHHHHHHENLYFQG) was cloned into the pBad vector (Invitrogen) behind the arabinose promoter. The His₆Mb was purified using Ni-chelation chromatography. Unmodified, recombinantly expressed sperm whale Mb (95-100 % pure in a 0.02 M Tris-Cl, pH 8 solution) was purchased from Sigma. Both protein samples were exchanged into PBS containing 50% (w/v) glycerol, added to reduce the background IR absorbance for the 2D IR experiments. For FT-IR and 2D IR experiments, the protein samples were concentrated to 7 mM, clarified through 45 μ m filters, and reduced with tenfold excess sodium dithionite. It has been shown that myoglobin does not form dimers at concentrations as high as 9 mM.(48) The possibility of dimer formation for His₆Mb will be discussed below. The protein samples were placed between two CaF₂ windows separated by a 50 μ m Teflon spacer. UV/visible and CD spectra of His₆Mb were also acquired in on a Cary 3E and Aviv 62A DS spectrometers, respectively.

Linear FT-IR spectra were acquired at 1 cm^{-1} resolution on a Bruker Vertex 70 spectrometer. The time-resolved infrared experiments were performed as previously described(29, 49) with 120 fs, \sim 5 μ J pulses at 1945 cm^{-1} generated with an ultrafast mid-IR laser system consisting of a Ti:Sapphire oscillator/regenerative amplifier pumped optical parametric amplifier. Briefly, the 2D IR echo experiments involved application of three mid-IR light pulses to the sample (\sim 0.8 μ J per pulse at the sample) with the times between the first and second pulse and the second and third pulse referred to as τ and T_w , respectively.(49) At a time $\leq \tau$ after the third pulse, a vibrational echo is emitted by the sample in a unique direction. The vibrational echo pulse is overlapped with another IR pulse, called the local oscillator, for heterodyne detection and to provide phase information for the vibrational echo signal. The combined vibrational echo/local oscillator pulse is passed through a

monochromator onto an IR array detector, which records a spectrum that yields the ω_m frequency axis (vertical axis), the axis of vibrational echo emission. Scanning τ produces an interferogram at each ω_m . These interferograms are then Fourier transformed to produce the second, ω_τ axis (horizontal axis) of the 2D IR spectrum. In the experiments, τ is scanned for fixed T_w to produce a 2D IR spectrum. T_w is then changed, and τ is again scanned to produce another 2D IR spectrum. The change in the spectra with T_w provides the dynamical information about the system.

Pump probe experiments are also performed to determine the vibrational lifetimes and for use in processing the 2D IR data. An $\sim 3.5 \mu\text{J}$ pump pulse is followed by a variably delayed, $\sim 0.4 \mu\text{J}$ probe pulse. The pump-induced changes in the probe beam spectrum at each time delay were measured by dispersing the transmitted probe beam through the monochromator onto the array detector.

C. Data Analysis

The linear FT-IR spectra were background-corrected by subtracting the solvent FT-IR spectrum, followed by fitting and subtracting a polynomial function to the spectral regions away from the CO band. This function was used to make small residual base line corrections. The resulting spectra were then fit to a sum of Gaussian functions. The time-resolved pump probe spectra were used to determine the vibrational lifetimes (T_1) of the CO in the His-tagged and unmodified Mb. At each frequency of a spectrum, the pump-induced difference in the probe beam intensity as function of the probe delay time was fit to an exponential decay.

Protein structural fluctuations cause the CO stretch frequency to evolve in time (spectral diffusion). The frequency-frequency correlation function (FFCF) connects the waiting time (T_w) dependent changes in the 2D band shapes caused by spectral diffusion to the time dependence of the structural changes of the proteins. The center line slope (CLS) method is used to determine the FFCF from 2D and linear spectra.(50, 51) This method provides an accurate way to extract the FFCF and also provides a useful quantity to plot.(50, 51) At a particular ω_τ , a slice through the 2D spectrum, projected onto the ω_m axis, is a spectrum with a peak at a particular ω_m value. Many such slices taken over a range of ω_τ values produce a set of points. Connecting the resulting points yields the center line. In the absence of a homogeneous contribution, at $T_w = 0$ the slope of the center line would be 1. At sufficiently long time, when spectral diffusion has sampled all frequencies within the absorption spectrum, the 2D IR line shape would be circular, and the center line would be horizontal with a slope of zero. It has been shown theoretically that the T_w -dependent part of the normalized FFCF is directly related to the T_w dependence of the slope of the center line. (50, 51) Thus the slope of the center line, the CLS, will vary between a maximum of 1 at $T_w = 0$ and 0 in the limit of sufficiently long waiting time. The presence of a homogeneous contribution to the spectrum causes the initial value of the slope to be less than 1 at $T_w = 0$ (see below).

The multiple time scale dynamics were modeled by a multiexponential form of the FFCF, $C(t)$.

$$C(t) = \sum_{i=1}^n \Delta_i^2 e^{-t/\tau_i} \quad (1)$$

For the i^{th} dynamical process, Δ_i is the range of CO frequencies sampled due to protein structural fluctuations, and τ_i is the time constant of these fluctuations. This form of the FFCF has been widely used and in particular found applicable in studies of the structural dynamics of heme-CO proteins.(12, 29, 32, 33, 45, 47, 52-54) The experimental time window is limited by the vibrational lifetime decay to several times T_1 , the vibrational lifetime, which reduces the signal to zero. Occurrence of very slow structural fluctuations on timescales longer than the experimental time window, if present, will appear as one of the $\tau_i = \infty$ in the FFCF. This term is referred to as the “static” component. The corresponding Δ_i is the amplitude of the static component, that is, the amplitude of the component of the fluctuations that are on a time scale long compared to the experimental time window.

If $\Delta\tau < 1$ for one component of the FFCF, then Δ and τ cannot be determined separately, but rather give rise to a motionally narrowed homogeneous contribution to the absorption spectrum with pure dephasing width given by $\Gamma = \Delta^2\tau = 1/\pi T_2^*$ where T_2^* is the pure dephasing time, and Γ is the pure dephasing linewidth. The total homogeneous dephasing time, T_2 , also has contributions from the vibrational lifetime. T_2 is given by

$$\frac{1}{T_2} = \frac{1}{T_2^*} + \frac{1}{2T_1}. \quad (2)$$

Detailed procedures for converting the CLS measurement into the FFCF have been described previously.(50, 51) By combining the CLS with the linear absorption spectrum, the full FFCF is obtained including the homogeneous component. Then using the vibrational lifetime, T_2^* and Γ are obtained from Equation 2.

III. Results and Discussion

The center frequency of the CO vibration in heme proteins is particularly sensitive to the local environment.(24-28) In MbCO, with the imidazole side group of the distal residue His64 in the pocket, there are two peaks, denoted A_1 and A_3 , that have been attributed to different configurations of the imidazole relative to the CO.(29, 31, 32) Figure 2 displays the FT-IR absorption spectrum of unmodified MbCO (panel A) and His₆MbCO (panel B) along with fits to a sum of Gaussians functions (dashed lines). The fit provides the center frequency and linewidth of the bands composing the spectra. As expected, the spectrum of unmodified MbCO contains two distinct overlapping bands, a very strong band at 1945 cm^{-1} (A_1 band) and a band at 1934 cm^{-1} (A_3 band) approximately half in total integrated area.

Comparing the spectra of Figure 2, the FT-IR spectra of His₆MbCO and MbCO appear almost identical. The His₆MbCO spectra shows two bands reflecting the A_1 and A_3 states with the same relative populations observed in the MbCO spectra. These two bands are believed to result from only a small change in the orientation of the side chain of His64, illustrating the high sensitivity of the FT IR spectrum to Mb heme pocket structure. The only difference observed in the His₆MbCO spectrum is a contribution from a very small band at 1964 cm^{-1} . While the band is clearly apparent and outside the spectral noise (see inset, Figure 2), it only constitutes 2% of the total integrated area of the spectrum. A band of similar frequency, denoted the A_0 state, is found in some Mb variants and when the sperm whale protein is in acidic conditions.(25, 55, 56) The A_0 state is believed to reflect a conformation in which a protonated His64 side chain is rotated out of the heme pocket. Thus, the FT-IR spectra indicate that the introduction of the His tag leads to very minor changes in the heme pocket environment, only slightly increasing the population of the A_0 structure. In comparison, FT IR spectra of mutant MbCO proteins show dramatic changes in

the frequencies and relative amplitudes of the composite bands.(57) Furthermore, no change in protein structure due to His tag incorporation is evident from the His₆MbCO UV/visible spectra, and the CD spectra is consistent with a largely helical protein (shown in Supporting Information).

2D IR spectra of MbCO and His₆MbCO were obtained for varying T_w times to examine the dynamics in presence and absence of the His tag (Figure 3). All spectra show peaks due to the 0-1 transitions along the diagonal (red) as well as negative peaks (blue), which arise from vibrational echo emission at the 1-2 transition frequencies and are shifted to lower frequency along the ω_m axis by the vibrational anharmonicity (25 cm^{-1}).^(47, 58-60) The key feature in this experiment is the change in the shape of the 0-1 bands in the 2D IR spectra as T_w is increased, as illustrated in Figure 3. As the structure of the protein evolves in time, the CO frequency changes (spectral diffusion) because its frequency is sensitive to the evolving protein structure. Previous experiments and simulations on MbCO and experiments on neuroglobin-CO have shown that the CO frequency fluctuations are sensitive to global protein structural dynamics.^(29-31, 54) At short T_w times (Figure 3), the peaks in the spectra are substantially elongated along the diagonal, reflecting the incomplete sampling of the inhomogeneous distribution of states contained in the absorption line shape. The peaks appear elongated along the diagonal because most of the CO molecules initially at frequencies ω_τ have the same final frequencies ω_m following the short T_w delay. The width perpendicular to the diagonal at very short T_w is caused by the motionally narrowed pure dephasing contribution with a small additional contribution from the vibrational lifetime. At longer T_w times, the protein has had time to sample more of its range of structures. The CO stretching mode no longer has the same initial (ω_τ) and final (ω_m) frequencies due to evolution of the protein structure during the time period T_w , and the bands in the spectra become less elongated along the diagonal (the major and minor axis are more similar).

To quantitatively compare the dynamics of the His-tagged and unmodified Mb, the CLS was determined from the A₁ band in the 2D IR spectra for each T_w .^(50, 51) Figure 4 shows the CLS vs. T_w for MbCO and His₆MbCO, as well as multiexponential fits to the data. As discussed in Section II, Experimental Procedures, the CLS decays were analyzed in combination with the linear FT-IR spectra and vibrational lifetimes to obtain the FFCFs, which quantify the dynamics associated with the fluctuating CO frequency caused by the structural dynamics of the protein. The parameters describing the FFCFs are listed in Table 1.

The ultrafast protein dynamics plus contributions from the solvent fluctuations produce a motionally narrowed Lorentzian (homogeneous) component of the absorption spectrum,⁽²⁹⁾ which is characterized by the pure dephasing time, T_2^* , and the pure dephasing linewidth, Γ . Both of these parameters are given in Table 1. Given that the two proteins have nearly identical FT-IR spectra, the initial smaller CLS value of the unmodified protein indicates a greater homogeneous contribution to the dynamics compared to the His-tagged protein. In accordance with this, determination of the FFCF yielded a homogeneous dephasing time of 3.8 ps for MbCO, while the FFCF of His₆MbCO showed a slower homogeneous dephasing time of 7.5 ps. The homogeneous dephasing time is thus influenced by the presence of the His tag; however, in both cases the homogeneous component is a minor contributor to the overall linewidth ($2\text{-}3\text{ cm}^{-1}$ of the 11 cm^{-1} linewidth). While the water/glycerol solvent contributes to the homogeneous dephasing, it is unlikely that the presence of the His tag changes the homogeneous dephasing because of its influence on the solvent dynamics per se. The protein is surrounded by solvent, and the fast motions of the solvent molecules gives rise to a component of the homogeneous dephasing by producing fluctuating electric fields at the CO. The presence of the His tag will at most make a difference to those solvent molecules in its immediate vicinity, which is a small fraction of all of the solvent. Most

likely the change in the homogeneous dephasing caused by the His tag comes about from changes in the very fast structural fluctuations of the protein itself, not from modification of the solvent.

On a slower timescale, fluctuations of the protein structure lead the CO to sample its possible IR frequencies (spectral diffusion). These dynamics are reflected in the T_w dependence of the CLS. For the unmodified protein, the CLS decay involves three timescales: a fast 1.4 ps component (τ_1), a slower 19 ps component (τ_2) and a very slow component that appears static on the experimental timescale ($\tau_3 = \infty$). The timescales differ from a previous 2D IR study of this protein.(31) However, in the current study, the solvent is 50 % glycerol/PBS as opposed to D₂O buffer used in the earlier study. The glycerol increases the viscosity six fold. The glycerol also reduces the solvent background and greatly improves the data quality. The result is that data could be acquired in this study to T_w of 80 ps while the previous data were measured to a T_w of 40 ps. Therefore the current study captures a larger range of the dynamics.

The perturbation of the dynamics of MbCO due to incorporation of the His tag is clear from inspection of the CLS decay curves in Figure 4 and the parameters given in Table 1. The CLS decay of His₆MbCO involves only two timescales: a 21 ps component (τ_2) and a very slow component that appears static on the experimental timescale ($\tau_3 = \infty$). Thus, the 1.4 ps dynamics of the unmodified protein are no longer observed when the His tag is introduced. The lack of this component is evident from inspection of the CLS decays curves at the shortest T_w times. The initial CLS decay of MbCO is much faster than the decay of His₆MbCO. The 1.4 ps component was still absent when experiments were performed with a protein concentration of 3 mM. Dimer formation is known to be absent at 7 mM for MbCO. (48) If dimer formation occurred for His₆MbCO at 7 mM, the reduction in concentration to 3 mM would reduce the dimer concentration by >5. The reduction in concentration lowered the viscosity of the sample by a factor of ~2, which caused a small decrease in the static component of the CLS, otherwise the curve was unchanged. Thus, dimer formation can be ruled out as the reason for the difference in dynamics between His₆MbCO and MbCO.

While the timescales of the slower dynamics are very similar, the amplitudes of the frequency fluctuations associated with the timescales differ somewhat between the two proteins. The Δ_2 for the two proteins are the same (2.7 cm⁻¹) for the native protein vs. the His-tagged protein (see Table 1). In contrast, the frequency fluctuation amplitude of the dynamics of the native protein on the slowest (>100s ps) timescale is less than that of His₆MbCO, 2.3 vs. 3.0 cm⁻¹, respectively. The observed similarity in timescales but variance in amplitudes is consistent with a situation where the His tag does not fundamentally change the nature of slower Mb motions. A possible explanation for the observed differences in the two proteins is that the faster (1.4 ps) motions of the native Mb slow upon His tag addition, leading to the removal of this contribution and increased amplitude of the slowest (>100s ps) timescale contribution to the FFCF of His₆MbCO.

Overall, the introduction of the His tag reduces the contributions to the FFCF from fast dynamics, both the very fast homogeneous dynamics and the T_w -dependent 1.4 ps dynamics, and alters the frequency fluctuation amplitudes associated with the slowest motions in MbCO. The influence of the His tag on the dynamics are surprising, as the addition to the protein is relatively small and placed at site distant from the bound CO (Figure 1). Given the similar FT-IR spectra of the modified and His-tagged Mb, the local structure within the heme pocket is not likely perturbed to a great extent by the His-tag. The A₁ band in particular showed the same center frequency and linewidth, suggesting the average electrostatic environment and the distribution of environments sampled by Mb in this conformation are unaltered by the His tag. Rather, the 2D IR data show that the His tag

changes the motions that lead Mb to sample the environments in the distribution. The differences in the amplitudes of the slowest (>100s ps) dynamics suggest that the His tag affects the global dynamics of Mb, consistent with previous molecular dynamics studies that found the FFCF to result from motions throughout Mb.(46)

IV. Concluding Remarks

This study addressed the general assumption that His tags are non-perturbative. While the His tag does not appear to have a dramatic impact on Mb structure, it does in a more subtle manner influence the Mb dynamics. In a recent survey of structures in the protein data bank, Carsons, et al. overall found no significant changes to protein structures due to the introduction of His tags.(13) However, slightly greater B factors, an indicator of greater structural disorder, were observed for His-tagged compared to the unmodified proteins, suggesting the protein dynamics may be altered. While resolved His tag structures are sometimes observed in crystal structures, more often the His tags are unresolved or unstructured, and assumed to be flopping about in solution. Such motion would be relatively slow, and if present in His₆MbCO, could contribute to the greater frequency fluctuation amplitude associated with the slowest motions. However, this type of His tag motion does not account for the loss of the fast 1.4 ps component observed in the native protein.

Several studies have observed adverse affects to protein structure or function due to interaction of the protein with the attached His tag. The effect of His tag incorporation on the structure and dynamics of the protein cytochrome *b*₅ was investigated in a recent study using molecular modeling and molecular dynamics simulations.(16) No disruption to the region surrounding the heme was observed, but a slight decreased RMSD was found in more distant regions of the protein due to stabilizing interactions between the protein with the His tag. In this case, the His tag adopts a helical structure that packs against the hydrophobic core of the protein through salt bridges, hydrogen bonding, and hydrophobic interactions. Similar types of interactions between a His tag and the enzyme tropinone reductase led to interference with enzymatic activity according to a recent experimental and molecular dynamics study.(14) Another investigation of His tag incorporation into the protein dynein found that stabilization of a particular helix through interaction with a His tag creates a new site for protein-protein binding.(15) In a similar manner, interactions between the His tag and Mb may lead to stabilization of a state that removes the contribution of 1.4 ps and faster protein motions to the FFCF.

Although the structural details of the observed changes in Mb dynamics at this point remain unknown, the results imply that caution should be used when studying the dynamics of His-tagged proteins or processes that depend on fast timescale structural fluctuations, such as the access of ligands into buried active sites(61), protein or ligand binding involving entropic changes(62, 63), or crossing a transition state in enzymatic catalysis(64, 65). In Mb, differences observed in the ps timescale geminate rebinding of O₂, NO, and CO suggest that motions on this fast timescale may be physiologically important for ligand discrimination.(66, 67) Although the 2D IR experimental data are limited in timescale by the vibrational lifetime of the CO probe, precluding determination of the exact timescales of the slowest, > 100s ps motions, the 2D IR data do show different frequency fluctuation amplitudes associated with the slowest motions. Thus, the CO experiences structural fluctuations on a > 100s ps timescale differently in the Mb variants, but we cannot determine how slow the associated motions are or whether the timescales differ. Data from other techniques sensitive to the protein structural details (e.g. those employing UV/visible and IR spectroscopy) may be influenced similarly.

This current study of dynamics corroborates those previous investigations that observed perturbations to structure,(16, 19, 21) folding,(17) and binding interactions with ligands(14, 18, 68) and protein partners(15, 20, 22, 23) due to His tag incorporation. In some cases His-tags appear to influence some but not all properties,(16, 19) in other cases their influence is position-dependent,(17, 19) further complicating the assessment of His tag perturbation. The significant differences in dynamics due to incorporation of a His tag in MbCO observed here using 2D IR spectroscopy, despite very similar FT-IR spectra, reveals that the perturbations may be subtle, and provides a general reason for caution in analyzing experimental data on His-tagged proteins.

Supplementary Material

Refer to Web version on PubMed Central for supplementary material.

References

1. Porath J. Immobilized metal ion affinity chromatography. *Protein Expression Purif.* 1992; 3:263–281.
2. Terpe K. Overview of tag protein fusions: From molecular and biochemical fundamentals to commercial systems. *Appl Microbiol Biotechnol.* 2003; 60:523–533. [PubMed: 12536251]
3. Lichty JJ, Malecki JL, Agnew HD, Michelson-Horowitz DJ, Tan S. Comparison of affinity tags for protein purification. *Protein Expression Purif.* 2005; 41:98–105.
4. Smith MC, Furman TC, Ingolia TD, Pidgeon C. Chelating peptide-immobilized metal ion affinity chromatography. A new concept in affinity chromatography for recombinant proteins. *J Biol Chem.* 1988; 263:7211–7215. [PubMed: 3284883]
5. Pedersen J, L C, Madsen MT, Dahl SW. Removal of n-terminal polyhistidine tags from recombinant proteins using engineered aminopeptidases. *Protein Expression Purif.* 1999; 15:389–400.
6. Jenny RJ, Mann KG, Lundblad RL. A critical review of the methods for cleavage of fusion proteins with thrombin and factor xa. *Protein Expression Purif.* 2003; 31:1–11.
7. Hao X, Cheng Y, Li-E C. Current strategies for polypeptide fusion tags removal. *Prog Biochem Biophys.* 2009; 36:1364–1669.
8. Vassiliev S, Lee CI, Brudvig GW, Bruce D. Structure-based kinetic modeling of excited-state transfer and trapping in histidine-tagged photosystem II core complexes from *Synechocystis*. *Biochemistry.* 2002; 41:12236–12243. [PubMed: 12356326]
9. Yao L, Vogeli B, Torchia DA, Bax A. Simultaneous NMR study of protein structure and dynamics using conservative mutagenesis. *J Phys Chem B.* 2008; 112:6045–6056. [PubMed: 18358021]
10. O'Sullivan DBD, Jones CE, Abdelraheim SR, Brazier MW, Toms H, Brown DR, Viles JH. Dynamics of a truncated prion protein, prp(113–231), from ¹⁵N NMR relaxation: Order parameters calculated and slow conformational fluctuations localized to a distinct region. *Protein Sci.* 2009; 18:410–423. [PubMed: 19173221]
11. Nienhaus K, Deng P, Belyea J, Franzen S, Nienhaus GU. Spectroscopic study of substrate binding to the carbonmonoxy form of dehaloperoxidase from *Amphitrite ornata*. *J Phys Chem B.* 2006; 110:13264–13276. [PubMed: 16805641]
12. Ishikawa H, Finkelstein IJ, Kim S, Kwak K, Chung JK, Wakasugi K, Massari AM, Fayer MD. Neuroglobin dynamics observed with ultrafast 2D-IR vibrational echo spectroscopy. *Proc Natl Acad Sci USA.* 2007; 104:16116–16121. [PubMed: 17916624]
13. Carson M, Johnson DH, McDonald H, Brouillette C, DeLucas LJ. His-tag impact on structure. *Acta Crystallogr Sect D Biol Crystallogr.* 2007; 63:295–301. [PubMed: 17327666]
14. Freydank AC, Brandt W, Dräger B. Protein structure modeling indicates hexahistidine-tag interference with enzyme activity. *Proteins: Struct Funct Bioinf.* 2008; 72:173–183.
15. Song J, Markley JL. Cautionary tail: The presence of an n-terminal tag on dynein light-chain roadblock/lc7 affects its interaction with a functional partner. *Protein Pept Lett.* 2007; 14:265–268. [PubMed: 17346231]

16. Lin YW, Ying TL, Liao LF. Molecular modeling and dynamics simulation of a histidine-tagged cytochrome. *J Mol Model*. 2010;1–8. [PubMed: 20306277]
17. Klose J, Wendt N, Kubald S, Krause E, Fechner K, Beyermann M, Bienert M, Rudolph R, Rothmund S. Hexa-histidin tag position influences disulfide structure but not binding behavior of in vitro folded n-terminal domain of rat corticotropin-releasing factor receptor type 2a. *Protein Sci*. 2004; 13:2470–2475. [PubMed: 15295109]
18. Emoto C, Murayama N, Wakiya S, Yamazaki H. Effects of histidine-tag on recombinant human cytochrome p450 3a5 catalytic activity in reconstitution systems. *Drug Metab Lett*. 2009; 3:207–211. [PubMed: 19702542]
19. Chant A, Kraemer-Pecore CM, Watkin R, Kneale GG. Attachment of a histidine tag to the minimal zinc finger protein of the *Aspergillus nidulans* gene regulatory protein area causes a conformational change at the DNA-binding site. *Protein Expression Purif*. 2005; 39:152–159.
20. Goel A, Colcher D, Koo JS, Booth BJM, Pavlinkova G, Batra SK. Relative position of the hexahistidine tag effects binding properties of a tumor-associated single-chain fv construct. *Biochim Biophys Acta, Gen Subj*. 2000; 1523:13–20.
21. Kim KM, Yi EC, Baker D, Zhang KYJ. Post-translational modification of the n-terminal his tag interferes with the crystallization of the wild-type and mutant sh3 domains from chicken src tyrosine kinase. *Acta Crystallographica Section D*. 2001; 57:759–762.
22. Amor-Mahjoub M, Suppini JP, Gomez-Vrielyunck N, Ladjimi M. The effect of the hexahistidine-tag in the oligomerization of hsc70 constructs. *J Chromatogr B*. 2006; 844:328–334.
23. Zhu ZC, Gupta KK, Slabbekoorn AR, Paulson BA, Folker ES, Goodson HV. Interactions between eb1 and microtubules: Dramatic effect of affinity tags and evidence for cooperative behavior. *J Biol Chem*. 2009; 284:32651–32661. [PubMed: 19778897]
24. Alben JO, Caughy WS. *Biochemistry*. 1968; 7:175–183. [PubMed: 5758542]
25. Li TS, Quillin ML, Phillips GN Jr, Olson JS. Structural determinants of the stretching frequency of CO bound to myoglobin. *Biochemistry*. 1994; 33:1433–1446. [PubMed: 8312263]
26. Park E, Andrews S, Boxer SG. Vibrational stark spectroscopy in proteins: A probe and calibration for electrostatic fields. *J Phys Chem*. 1999; 103:9813–9817.
27. Phillips GN Jr, Teodoro MN, Li T, Smith B, Olson JS. Bound CO is a molecular probe of electrostatic potential in the distal pocket of myoglobin. *J Phys Chem B*. 1999; 103:8817–8829.
28. Spiro TG, Wasbotten IH. CO as a vibrational probe of heme protein active sites. *J Inorg Biochem*. 2005; 99:34–44. [PubMed: 15598489]
29. Merchant KA, Noid WG, Akiyama R, Finkelstein I, Goun A, McClain BL, Loring RF, Fayer MD. Myoglobin-CO substate structures and dynamics: Multidimensional vibrational echoes and molecular dynamics simulations. *J Am Chem Soc*. 2003; 125:13804–13818. [PubMed: 14599220]
30. Merchant KA, Noid WG, Thompson DE, Akiyama R, Loring RF, Fayer MD. Structural assignments and dynamics of the A substates of MbCO: Spectrally resolved vibrational echo experiments and molecular dynamics simulations. *J Phys Chem B*. 2003; 107:4–7.
31. Bagchi S, Nebgen BT, Loring RF, Fayer MD. Dynamics of a myoglobin mutant enzyme: 2D-IR vibrational echo experiments and simulations. *J Am Chem Soc*. 2010; 132:18367–18376. [PubMed: 21142083]
32. Merchant KA, Thompson DE, Xu QH, Williams RB, Loring RF, Fayer MD. Myoglobin-CO conformational substate dynamics: 2d vibrational echoes and md simulations. *Biophys J*. 2002; 82:3277–3288. [PubMed: 12023251]
33. Kim S, Chung JK, Kwak K, Bowman SE, Bren KL, Bagchi B, Fayer MD. Native and unfolded cytochrome *c*-comparison of dynamics using 2D-IR vibrational echo spectroscopy. *J Phys Chem B*. 2008; 112:10054–10063. [PubMed: 18646797]
34. Ishikawa H, Kwak K, Chung JK, Kim S, Fayer MD. Direct observation of fast protein conformational switching. *Proc Natl Acad Sci USA*. 2008; 105:8619–8624. [PubMed: 18562286]
35. Thielges MC, Chung JK, Fayer MD. Protein dynamics in cytochrome p450 molecular recognition and substrate specificity using 2D IR vibrational echo spectroscopy. *J Am Chem Soc*. 2010; 133:3995–4004. [PubMed: 21348488]

36. Bagchi S, Thorpe DG, Thorpe IF, Voth GA, Fayer MD. Conformational switching between protein substates studied with 2D IR vibrational echo spectroscopy and molecular dynamics simulations. *J Phys Chem B*. 2010; 114:17187–17193. [PubMed: 21128650]
37. Hill JR, Tokmakoff A, Peterson KA, Sauter B, Zimdars DA, Dlott DD, Fayer MD. Vibrational dynamics of carbon monoxide at the active site of myoglobin: Picosecond infrared free-electron laser pump-probe experiments. *J Phys Chem*. 1994; 98:11213–11219.
38. Rella CW, Rector KD, Kwok AS, Hill JR, Schwettman HA, Dlott DD, Fayer MD. Vibrational echo studies of myoglobin-CO. *J Phys Chem*. 1996; 100:15620–15629.
39. Rector KD, Rella CW, Kwok AS, Hill JR, Sligar SG, Chien EYP, Dlott DD, Fayer MD. Mutant and wild type myoglobin-CO protein dynamics: Vibrational echo experiments. *J Phys Chem B*. 1997; 101:1468–1475.
40. Rector KD, Fayer MD. Vibrational echoes: A new approach to condensed matter vibrational spectroscopy. *Intl Rev Phys Chem*. 1998; 17:261–306.
41. Rector KD, Fayer MD. Myoglobin dynamics measured with vibrational echo experiments. *Laser Chem*. 1999; 19:19–34.
42. Rector KD, Thompson DE, Merchant K, Fayer MD. Dynamics in globular proteins: Vibrational echo experiments. *Chem Phys Lett*. 2000; 316:122–128.
43. Merchant KA, Thompson DE, Fayer MD. Two-dimensional time-frequency ultrafast infrared vibrational echo spectroscopy. *Phys Rev Lett*. 2001; 86:3899–3902. [PubMed: 11329352]
44. Merchant KA, Xu QH, Thompson DE, Fayer MD. Frequency selected ultrafast infrared vibrational echo studies of liquids, glasses and proteins. *J Phys Chem A*. 2002; 106:8839–8849.
45. Finkelstein IJ, Goj A, McClain BL, Massari AM, Merchant KA, Loring RF, Fayer MD. Ultrafast dynamics of myoglobin without the distal histidine: Stimulated vibrational echo experiments and molecular dynamics simulations. *J Phys Chem B*. 2005; 109:16959–16966. [PubMed: 16853158]
46. Massari AM, Finkelstein IJ, McClain BL, Goj A, Wen X, Bren KL, Loring RF, Fayer MD. The influence of aqueous vs. Glassy solvents on protein dynamics: Vibrational echo experiments and molecular dynamics simulations. *J Am Chem Soc*. 2005; 127:14279–14289. [PubMed: 16218622]
47. Finkelstein IJ, Zheng J, Ishikawa H, Kim S, Kwak K, Fayer MD. Probing dynamics of complex molecular systems with ultrafast 2D IR vibrational echo spectroscopy. *Phys Chem Chem Phys*. 2007; 9:1533–1549. [PubMed: 17429547]
48. Minton AP, Lewis MS. Self-association in highly concentrated-solutions of myoglobin - a novel analysis of sedimentation equilibrium of highly nonideal solutions. *Biophys Chem*. 1981; 14:317–324. [PubMed: 7337804]
49. Park S, Kwak K, Fayer MD. Ultrafast 2D-IR vibrational echo spectroscopy: A probe of molecular dynamics. *Laser Phys Lett*. 2007; 4:704–718.
50. Kwak K, Park S, Finkelstein IJ, Fayer MD. Frequency-frequency correlation functions and apodization in 2D-IR vibrational echo spectroscopy, a new approach. *J Chem Phys*. 2007; 127:124503. [PubMed: 17902917]
51. Kwak K, Rosenfeld DE, Fayer MD. Taking apart 2D-IR vibrational echo spectra: More information and elimination of distortions. *J Chem Phys*. 2008; 128:204505. [PubMed: 18513030]
52. Finkelstein IJ, Ishikawa H, Kim S, Massari AM, Fayer MD. Substrate binding and protein conformational dynamics measured via 2D-IR vibrational echo spectroscopy. *Proc Natl Acad Sci USA*. 2007; 104:2637–2642. [PubMed: 17296942]
53. Massari AM, Finkelstein IJ, Fayer MD. Dynamics of proteins encapsulated in silica sol-gel glasses studied with IR vibrational echo spectroscopy. *J Am Chem Soc*. 2006; 128:3990–3997. [PubMed: 16551107]
54. Ishikawa H, Kim S, Kwak K, Wakasugi K, Fayer MD. Disulfide bonds' influence on protein structural dynamics probed with 2D-IR vibrational echo spectroscopy. *Proc Natl Acad Sci USA*. 2007; 104:19309–19314. [PubMed: 18042705]
55. Shimada H, Caughey WS. Dynamic protein structures. *J Biol Chem*. 1982; 257:1893–1900.
56. Morikis D, Champion PM, Springer BA, Sligar SG. Resonance raman investigations of site-directed mutants of myoglobin - effects of distal histidine replacement. *Biochemistry*. 1989; 28:4791–4800. [PubMed: 2765511]

57. Li T, Quillin ML, Phillips GN Jr, Olson JS. Structural determinants of the stretching frequency of CO bound to myoglobin. *Biochemistry*. 1994; 33:1433–1446. [PubMed: 8312263]
58. Tokmakoff A, Kwok AS, Urdahl RS, Francis RS, Fayer MD. Multilevel vibrational dephasing and vibrational anharmonicity from infrared photon echo beats. *Chem Phys Lett*. 1995; 234:289–295.
59. Rector KD, Kwok AS, Ferrante C, Tokmakoff A, Rella CW, Fayer MD. Vibrational anharmonicity and multilevel vibrational dephasing from vibrational echo beats. *J Chem Phys*. 1997; 106:10027–10036.
60. Golonzka O, Khalil M, Demirdoven N, Tokmakoff A. Vibrational anharmonicities revealed by coherent two-dimensional infrared spectroscopy. *Phys Rev Lett*. 2001; 86:2154–2157. [PubMed: 11289878]
61. Ruscio JZ, Kumar D, Shukla M, Prisant MG, Murali TM, Onufriev AV. Atomic level computational identification of ligand migration pathways between solvent and binding site in myoglobin. *Proc Natl Acad Sci USA*. 2008; 105:9204–9209. [PubMed: 18599444]
62. Frederick KK, Marlow MS, Valentine KG, Wand AJ. Conformational entropy in molecular recognition by proteins. *Nature*. 2007; 448:325–U323. [PubMed: 17637663]
63. Stone MJ. NMR relaxation studies of the role of conformational entropy in protein stability and ligand binding. *Acc Chem Res*. 2001; 34:379–388. [PubMed: 11352716]
64. Zhong DP. Ultrafast catalytic processes in enzymes. *Curr Opin Chem Biol*. 2007; 11:174–181. [PubMed: 17353141]
65. Roca M, Moliner V, Tunon I, Hynes JT. Coupling between protein and reaction dynamics in enzymatic processes: Application of grote-hynes theory to catechol o-methyltransferase. *J Am Chem Soc*. 2006; 128:6186–6193. [PubMed: 16669689]
66. Brunori M, Bourgeois D, Vallone B. The structural dynamics of myoglobin. *J Struct Biol*. 2004; 147:223–234. [PubMed: 15450292]
67. Olson JS, Phillips GN. Kinetic pathways and barriers for ligand binding to myoglobin. *J Biol Chem*. 1996; 271:17593–17596. [PubMed: 8698688]
68. Fonda I, Kenig M, Gaberc-Porekar V, Pristovaek P, Menart V. Attachment of histidine tags to recombinant tumor necrosis factor-alpha drastically changes its properties. *Sci World J*. 2002; 2:1312–1325.

Abbreviations

MbCO	myoglobin-CO
His₆MbCO	His tag-myoglobin-CO
FFCF	frequency-frequency correlation function
CLS	center line slope

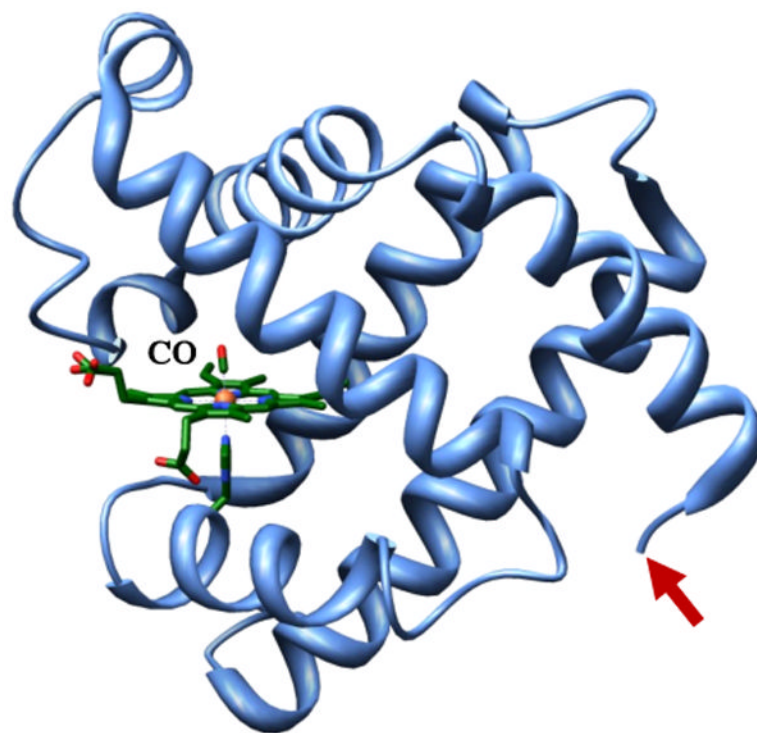


Figure 1.
Structure of sperm whale myoglobin (pdb 1bzt) with bound CO ligand. Site of N-terminal His₆ affinity tag placement shown by red arrow.

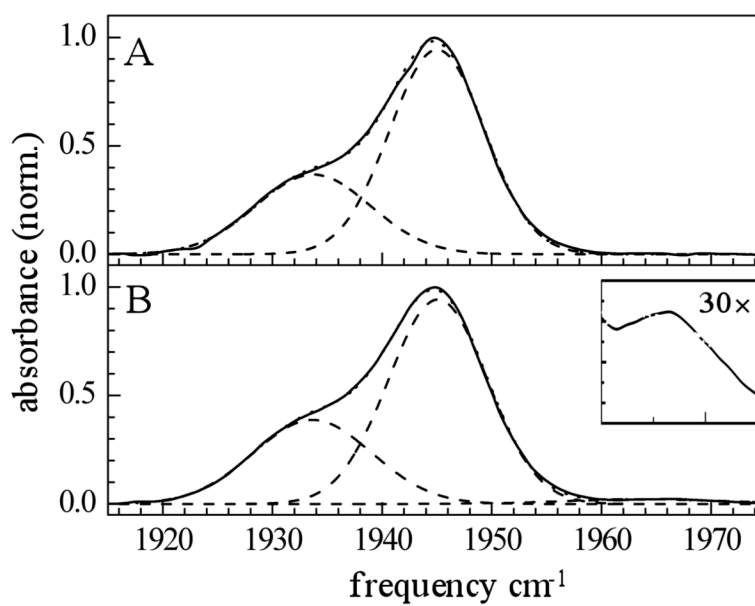


Figure 2. FT-IR spectra of (A) MbCO and (B) His₆MbCO. Gaussian fits are shown as dashed lines. The inset in (B) shows a 30X expanded view (1960-1975 cm⁻¹) of the A₀ band.

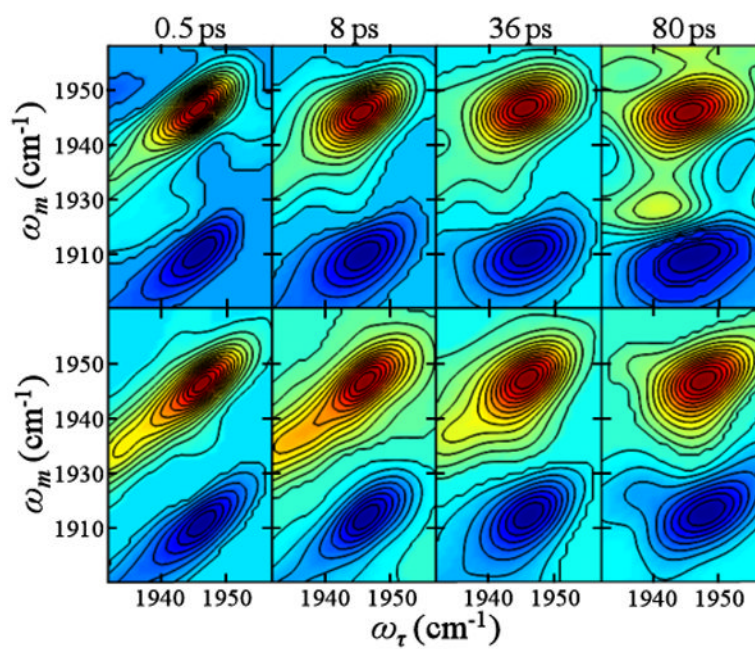


Figure 3. 2D IR spectra of MbCO (upper panels) and His₆MbCO (lower panels) for various T_w times. A total of 20 contour lines are shown.

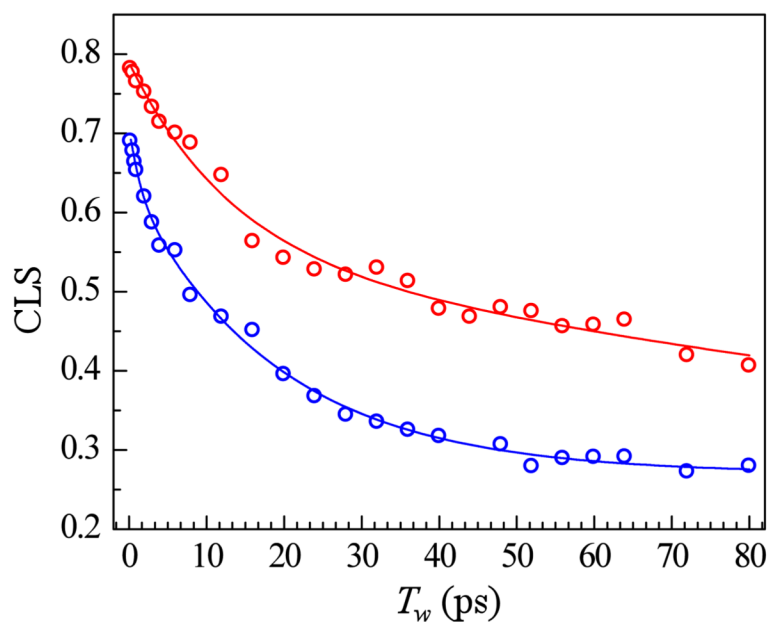


Figure 4. CLS decay curves and corresponding exponential fits for MbCO (blue) and His₆MbCO (red).

Table 1
Dynamic Parameters from 2D IR Spectra

	MbCO	His₆MbCO
T_1 (ps)	17	20
T_2^* (ps)	3.8	7.3
Γ (cm ⁻¹)	2.8	1.5
τ_1 (ps)	1.4	NA
Δ_1 (cm ⁻¹)	1.2	NA
t_2 (ps)	19	21
Δ_2 (cm ⁻¹)	2.7	2.7
t_3 (ps)	∞	∞
Δ_3 (cm ⁻¹)	2.3	3.0